Ocean Sci. Discuss., 8, 1403–1440, 2011
www.ocean-sci-discuss.net/8/1403/2011/
doi:10.5194/osd-8-1403-2011

Ocean Science Discussions

Wind forcing of salinity anomalies in the Denmark Strait overflow

S. Hall[1,2], **S. R. Dye**[2], **K. J. Heywood**[1], **and M. R. Wadley**[3]

[1]School of Environmental Sciences, University of East Anglia, Norwich, UK
[2]Centre for Environment, Fisheries and Aquaculture Science (Cefas), Lowestoft, UK
[3]School of Mathematics, University of East Anglia, Norwich, UK

Received: 20 May 2011 – Accepted: 10 June 2011 – Published: 21 June 2011

Correspondence to: K. J. Heywood (k.heywood@uea.ac.uk)

Published by Copernicus Publications on behalf of the European Geosciences Union.

Abstract

The overflow of dense water from the Nordic Seas to the North Atlantic through Denmark Strait is an important part of the global thermohaline circulation. The salinity of the overflow plume has been measured by an array of current meters across the continental slope off the coast of Angmagssalik, southeast Greenland since September 1998. During 2004 the salinity of the overflow plume changed dramatically, with the entire width of the array (70 km) freshening between January 2004 and July 2004, with a significant negative salinity anomaly of about 0.06 in May. The event in May represents a fresh anomaly of over 3 standard deviations from the mean since recording began in 1998. We show that the OCCAM 1/12° Ocean General Circulation Model not only reproduces the 2004 freshening event ($r = 0.96$, $p < 0.01$), but also correlates well with salinity observations over a previous 6 year period ($r = 0.54$, $p < 0.01$). Consequently the physical processes causing the 2004 anomaly and prior variability in salinity are investigated using the model output. Our results reject the hypotheses that the anomaly is caused by processes occurring between the overflow sill and the moorings, or by an increase in upstream net freshwater input. Instead, we show that the 2004 salinity anomaly is caused by an increase in volume flux of low salinity water, with a potential density greater than 27.60 kg m^{-3}, flowing towards the Denmark Strait sill in the East Greenland Current. This is caused by an increase of southward wind stress upstream of the sill at around 75° N 20° W four and a half months earlier, and an associated spin-up of the Greenland Sea Gyre.

1 Introduction

The overflow of cold, dense water from the Nordic Seas to the Atlantic Ocean across the Greenland-Scotland Ridge is an important component of the global thermohaline circulation. The total overflow is about 6 Sv (1 Sv = 10^6 m^3 s^{-1}), with roughly half of this passing through Denmark Strait, and the other half passing east of Iceland mainly

OSD

8, 1403–1440, 2011

through the Faroe Bank Channel (Dickson and Brown, 1994; Hansen and Østerhus, 2000). Intense mixing immediately downstream of the Denmark Strait overflow sill (Fig. 1) induces strong entrainment of ambient Atlantic waters into the overflow plume (Voet and Quadfasel, 2010), which flows southwards along the Greenland continental slope into the deep North Atlantic as Denmark Strait Overflow Water (DSOW). DSOW is typically identified as having a potential density greater than 27.8 $\mathrm{kg\,m^{-3}}$ (Dickson and Brown, 1994; Saunders, 2001). For convenience, values of potential density will be quoted without units for the remainder of this paper. This system of overflow and entrainment is the main contributor to North Atlantic Deep Water (NADW), the deep limb of the global thermohaline circulation (Dickson and Brown, 1994). In addition to DSOW, the surface waters of the East Greenland Current (EGC) also flow south through Denmark Strait, and Pickart et al. (2005) have identified a separate southward flowing current formed from dense water cascading over the East Greenland shelf edge south of the sill, known as the East Greenland Spill Jet. The purpose of this paper is to establish the cause of observed salinity anomalies in DSOW.

The source of DSOW is still an open question, but the EGC, and currents originating in the Iceland Sea, are widely recognised as the main pathways for different DSOW sources to reach the overflow sill (Rudels et al., 2002; Jónsson and Valdimarrson, 2004; Köhl, 2010) (Fig. 1). Any changes to the proportion of each constituent source water mass making up the total overflow just north of the sill, or a modification to the salinity characteristics of those water masses, have the potential to impact the salinity of the deep overflow. A long-term freshening trend and interannual fresh anomalies at the overflow have previously been attributed to an increase in freshwater input to the Nordic Seas from higher net precipitation, sea-ice melt and glacial run-off (Dickson et al., 2002; Curry et al., 2003; Peterson et al., 2006). However, most studies so far have implicated changes to the proportions of each water mass comprising the overflow as the main cause of observed salinity anomalies downstream of Denmark Strait, driven by changes in the local wind forcing. Rudels et al. (2002) reported that in 1990, increased wind-driven mixing resulted in a larger volume flux from the Iceland

Sea, causing fresher and colder DSOW. They argue that it is the final mixing just north of Denmark Strait which sets the DSOW characteristics by changing the contributions from the different water masses involved in the DSOW formation. Rudels et al. (2003), by comparing water masses derived from hydrographic observations upstream of Denmark Strait, show that on time scales from months to years, wind forcing variability determines whether the DSOW originates from either the Iceland Sea or the EGC.

More recently, Holfort and Albrecht (2007) argued that salinity anomalies in the overflow are driven by changes in the local wind forcing, based upon significant correlations between DSOW salinity and the wind stress west and north of Iceland. They speculated that stronger southward winds could result in a greater volume of low salinity water flowing from the north towards Denmark Strait in the EGC, with a lesser volume of higher salinity Recirculating Atlantic Water (RAW) present immediately upstream of the sill.

Our study identifies and assesses several possible mechanisms responsible for salinity anomalies in the overflow plume downstream of the sill, and investigates the likely contribution from each mechanism. Hypotheses are formulated and tested using a combination of observational data, reanalysis, and an appropriate Ocean General Circulation Model (OGCM). Section 2 provides an overview of the observational data used for this study and states the hypotheses to be tested. Section 3 introduces the OGCM and demonstrates its ability to represent the variability of the Denmark Strait overflow. Hypotheses are tested in Sects. 4, 5 and 6 and the results discussed, and a summary is given in Sect. 7.

2 Salinity time series at the Angmagssalik moorings

Since 1986 the Centre for Environment, Fisheries and Aquaculture Science (Cefas) in the UK, with colleagues in Germany (University of Hamburg) and Finland (Finnish Institute of Marine Research), have instrumented the core of the overflow plume 500 km south of Denmark Strait at Angmagssalik, as part of various EU-funded projects

OSD
8, 1403–1440, 2011

including Variability of Exchanges in the Northern Seas (VEINS), Arctic-Subarctic Ocean Fluxes (ASOF) and Developing Arctic Modelling and Observing Capabilities for Long-Term Environmental Studies (DAMOCLES) (Dickson and Brown, 1994; Dickson et al., 2008). Typically, a “picket fence” array of 7 or 8 current meter moorings is deployed annually, normal to the southeast Greenland Slope to intercept the descending overflow plume (Fig. 1, Sect. AB). Initially, only current velocity and temperature were monitored (Dickson and Brown, 1994), but from 1998 onwards, a variable number of SBE-37 MicroCAT salinity sensors were also deployed across the array (Table 1).

For this investigation, salinity time series from four moorings F2, UK1, G1 and UK2 are analysed (Dickson et al., 2008). These instruments are located at depths of 1760 m, 1970 m, 2180 m and 2350 m respectively (Table 1). Fig. 2a shows a vertical section through the moorings, with potential density and salinity obtained from CTD casts during the June 2009 R/V *Maria S. Merian* 12-1 cruise (Quadfasel, 2009). The salinity and density are typical for the overflow 500 km south of the sill (Dickson and Brown, 1994). The bottom water mass, which forms the core of the overflow, is DSOW, characterised by a potential density greater than 27.85 and salinity less than 34.9 (Dickson and Brown, 1994; Pickart et al., 2005). Between a depth of about 1500 m and the 27.85 isopycnal lies Iceland Scotland Overflow Water (ISOW), which is the overflow water entering the North Atlantic through the Faroe Bank Channel. This circulates round the Reykjanes Ridge (Fig. 1) into the Irminger Basin, and usually has a potential density greater than 27.8 and salinity 34.91 to 34.93 (Fogelqvist et al., 2003). The 27.8 isopycnal separates ISOW from the overlying Labrador Sea Water (LSW), formed by wintertime convection in the Labrador and Irminger Seas (Walter et al., 2005). The upper limit of LSW occurs at a depth of about 500 m, where the 27.70 isopycnal separates the surface and deep water masses (Holliday et al., 2007). The moorings are positioned directly in the core of the dense overflow, ideal for monitoring the temporal variability of DSOW salinity (Fig. 2a). Salinity values have been calibrated against CTD data obtained at the start and end of each mooring deployment. No long-term drift was detected in any of the instruments. Data were binned into 1 h means from

OSD
8, 1403–1440, 2011

the original 10 min sampling rate, and tidal signals were removed using the T_TIDE MATLAB harmonic analysis toolbox (Pawlowicz, 2002) (Fig. 3).

Strong interannual variation is evident, with fresh anomalies passing through the overflow core in the early months of most years. In particular there is a temporary reduction in salinity of around 0.04 between January 2004 and July 2004, peaking at 0.06 in May 2004. The May 2004 event represents a change of around 3 standard deviations of hourly values from the 1998 to 2005 mean of 34.87. Moreover, this event is identified at 3 of the adjacent moorings spanning a distance of about 40 km, so malfunction in a single instrument can be eliminated as a cause. This also suggests that the fresh anomaly is unlikely to have been caused by a shift in the position of the entire overflow plume across the continental slope, because each mooring would measure a different value for salinity as the plume changed position and encompassed more or fewer of the moorings. In addition, Fig. 2a, which is a snapshot of the salinity in June 2009 shows the overflow plume coincident with the moorings, implying minimal temporal variability in the position of the plume at the moorings. The early 1999 fresh event is similar in magnitude to the 2004 anomaly, but shorter in duration, extending between March and June. It was only recorded by the one available mooring (UK1). A similar mechanism could be responsible in both cases. Although the negative anomalies all appear in the first half of each year, they do not all occur during the same months and are of significantly varying amplitude. Fourier analysis shows the seasonal cycle to be negligible and therefore we have not removed a seasonal cycle from the salinity time series.

The salinity time series (Fig. 3) also displays high, but not dominant, variability over periods of 4 to 10 days. Dickson and Brown (1994) analysed current and temperature records at the Angmagssalik array, and found similar, though dominating, variability on timescales of 1 to 12 days. This is caused by mesoscale eddies passing through the moorings. To remove these, a first order low-pass Butterworth filter with a cut-off frequency of 1/30 days^{-1} was applied to the salinity time series. To produce a continuous salinity time series between August 2000 and July 2005, G1 salinity data

OSD
8, 1403–1440, 2011

were used to fill the gap in the UK1 time series between July 2001 and June 2002 (Fig. 3). UK1 and G1 are adjacent in the array, and display almost identical values of salinity (Fig. 3). The correlation coefficient between the two filtered time series for August 2000 to July 2001 is 0.91 ($p < 0.01$), so we can be confident that G1 and UK1 are monitoring the same flow.

Based on the current understanding of how the source of the overflow originates upstream of the sill, and the nature of its descent towards the North Atlantic (Dickson and Brown, 1994; Rudels et al., 2002), we formulate three hypotheses (H1, H2 and H3) to explain the cause of the 2004 negative salinity anomaly at Angmagssalik. H2 is broken down into three sub-hypotheses (H2a, H2b and H2c).

- H1 – the 2004 anomaly resulted from processes occurring between the overflow sill and the moorings associated with anomalous mixing or water mass pathways.
- H2 – the 2004 anomaly was caused by a change in salinity of the source waters feeding the overflow at the sill.
- H2a – the 2004 anomaly originated from glacial ice melt anomalies upstream of the sill.
- H2b – the 2004 anomaly originated from precipitation anomalies upstream of the sill.
- H2c – the 2004 anomaly originated from sea-ice melt anomalies upstream of the sill.
- H3 – the 2004 anomaly was caused by changes in the proportion of different source waters feeding the overflow.

Hypotheses H1 and H2 will be tested using the output from an OGCM, and H3 using the reanalysis data which force the model.

Discussion Paper | Discussion Paper | Discussion Paper | Discussion Paper |

OSD
8, 1403–1440, 2011

Wind forcing of salinity anomalies in the Denmark Strait overflow

S. Hall et al.

3 The Ocean Circulation and Climate Advanced Modelling (OCCAM) model

The OGCM selected is the Ocean Circulation and Climate Advanced Modelling (OCCAM) model. The OCCAM model (run by the National Oceanography Centre, Southampton) is a high resolution, primitive equation global OGCM with a 1/12° horizontal resolution, and 66 vertical layers of progressively increasing thickness from 5 m near the surface to 200 m in the deep ocean (http://www.noc.soton.ac.uk/JRD/OCCAM; Coward and de Cuevas, 2005). The model has a rotated grid over the North Atlantic, and is forced with 6-hourly zonal and meridional 10 m wind stress from the National Centres for Environmental Prediction (NCEP) global reanalysis (Kalnay et al., 1996). It also incorporates a free surface, partial bottom cell scheme and sea-ice model. Its ability to represent boundary currents, frontal systems and eddy fields, combined with an accurate representation of small scale topographic features and sea-ice behaviour, makes it an ideal tool to examine the dynamical processes occurring in and upstream of Denmark Strait. The layered depth structure can limit the ability of OCCAM to correctly reproduce vertical mixing, which may result in an unrealistic representation of the overflow plume as it descends from the sill to the moorings (Saunders et al., 2008). However, processes upstream of the sill which predominantly determine DSOW properties mainly occur in the highly resolved top 600 m of the water column, so this limitation of OCCAM should not significantly reduce its suitability for use in this study. Five-day means from OCCAM run 401 were obtained for the period January 1988 to December 2004. Some long-term drift is present in temperature and salinity during model spin-up between 1988 and 1993, but is negligible thereafter.

Before using OCCAM as a tool to examine the causes of salinity anomalies at the moorings, it must be demonstrated that OCCAM represents the basic structure and temporal evolution of the dense overflow. If so, it is likely that the mechanisms driving the variability at Angmagssalik are also present in the model.

Firstly, we examine the mean June salinity and density between 1994 and 2004, across a section in OCCAM equivalent to the location of the Angmagssalik array

OSD
8, 1403–1440, 2011

(Fig. 2b), and compare results with those observed (Fig. 2a). Mean OCCAM June salinity and density (Fig. 2b) show similar structure to the observations (Fig. 2a), with relatively high salinity water overlying denser, less saline water at the bottom of the water column (note the different colour scales for each figure). Salinity values from the CTD data range from about 35 in the top 500 m, to minimum values of around 34.9 in the core of the overflow (Fig. 2a), and density increases from less than 27.7 at the surface to 27.85 bounding the overflow core. OCCAM also identifies a salinity minimum of around 34.9, bounded by the 27.8 isopycnal, positioned about 80 km further down the slope than in Fig. 2a, but still encompassing roughly half of the moorings (Fig. 2b). The main difference occurs in the top 1500 m of the water column, where salinity in OCCAM is around 0.2 higher than the observations, and density is around 0.1 lower (Fig. 2b). This should not impair our investigation, because we are concerned with temporal variability of salinity anomalies, not absolute values.

Secondly, we conduct zero time-lagged regression analysis between UK1 salinity anomaly time series, and OCCAM salinity anomaly time series in each grid cell across the same section (Fig. 4). To maintain consistency between both time series, the UK1 data were binned into 5-day means and the time series truncated to 31 December 2004, and a first order low-pass Butterworth filter with a cut-off frequency of 1/30 days^{-1} was applied to the OCCAM data. In addition, the 1994 to 2004 mean of OCCAM current velocity vectors perpendicular to section AB were also extracted.

Figure 4 clearly identifies the high velocity core of the overflow, with a maximum mean velocity of about 30 cm s^{-1} in the centre of the core, reducing to about 5 cm s^{-1} at the outer edge of the overflow. The overflow core extends from a depth of 500 m to 1500 m, with a width of about 35 km, tightly hugging the East Greenland continental slope. Its location is bounded by the 27.6 and 27.7 isopycnals (Fig. 2b). With respect to velocity, the OCCAM overflow is in very good agreement with data obtained from the Angmagssalik moorings, which range from around 20 to 40 cm s^{-1} (Dickson and Brown, 1994). However, the spatial representation of the overflow is less consistent with field observations. Firstly, the mooring data show the core of the overflow to be a much broader structure than that suggested by the model in Fig. 4, encompassing the whole of the mooring array (Fig. 2a). Secondly, the overflow is recognised as having a density greater than 27.8, and salinity less than 34.9 (Dickson and Brown, 1994). While this definition is supported by the observational data in Fig. 2a, OCCAM identifies the density of the overflow as being about 27.65, and does not show the overflow core coinciding with the freshest water, instead the salinity of the overflow core is about 35.2. This is due to the poor ability of the model to accurately represent vertical mixing processes, which occur as the plume makes its rapid descent from the sill. That said, the overflow plume is clearly present in OCCAM, displaying the correct velocity, and in the approximate vicinity of the moorings. More importantly for this study, a region of coherent, high correlation exists between UK1 mooring salinity and OCCAM salinity, corresponding almost exactly with the region of highest velocity (Fig. 4). At the position marked "X" on Fig. 4, the correlation coefficient for the whole time series was 0.54 ($p < 0.01$), and increased to 0.96 ($p < 0.01$) for 2004 only (Fig. 5a), implying that this region in OCCAM is responding to the same dynamical process influencing the overflow salinity as the ocean. This makes it a suitable tool for understanding the underlying mechanisms responsible for causing the 2004 anomaly at Angmagssalik.

4 Testing of hypothesis H1

If it can be demonstrated that OCCAM identifies the anomaly at the overflow sill, on the correct density layer, and with a time-lag equivalent to the transit time for this water to travel between the sill and the moorings, this would strongly suggest that processes upstream of the sill are responsible for causing the anomaly at the moorings. It would also signify that it is unlikely to be mechanisms occurring between the sill and the moorings, such as entrainment and mixing with ISOW and LSW that are producing the anomaly. Hence in that case the anomaly must form upstream of the sill, and advect from the sill to the moorings in the dense overflow, meaning that hypothesis H1 might be rejected.

OSD
8, 1403–1440, 2011

Wind forcing of salinity anomalies in the Denmark Strait overflow

S. Hall et al.

A time-lagged regression analysis was performed between the UK1 salinity anomaly time series and OCCAM salinity anomaly time series in each grid cell across a section through the sill. Fig. 6 clearly shows a region of coherent, high correlation between time series of UK1 mooring salinity anomaly and OCCAM salinity anomaly, between depths of about 150 m to 350 m, and 60 km to 180 km from the Greenland coast. The highest correlation coefficient was 0.67 ($p < 0.01$) (marked "+" on Fig. 6), and occurred at a time lag of 6 weeks (Fig. 5b). Its location just beneath the 27.6 isopycnal, corresponds closely with the value of 27.65 obtained for the density of the core of the overflow in OCCAM (Fig. 2b). This implies that water at the sill, at the location marked "+" on Fig. 6, is probably the same water causing the anomaly at the moorings.

Although both time series in Fig. 5b display similar temporal variability, the amplitude of the anomalies at the sill in OCCAM is around 10 times that of mooring UK 1 (Fig. 5b). This could indicate that mixing and entrainment with surrounding water masses, which occur as the overflow plume descends the slope, dilute the anomaly to one tenth of its amplitude at the sill, by the time it reaches the moorings. To test this, a passive tracer experiment was performed "off-line" using the OCCAM velocity and density fields to force the advection and diffusion equations for the tracer. The tracer was initialised at the sill in OCCAM, at grid cells within the density range 27.6 to 27.8, to correspond with the density of the water at location "+" in Fig. 6. A continuous release was used to permit the concentration of tracer downstream of the sill to stabilise over time, rather than be quickly flushed out of the system. The tracer was released continuously from 12 December 2003, to allow enough time for the concentration of tracer at the moorings to stabilise before the arrival of the anomaly in May 2004.

Figure 7 shows a time series of tracer concentration taken from the grid cell representing the core of the overflow in OCCAM at the moorings (marked "X" in Fig. 4). The tracer arrives at the moorings around 6 weeks following its release at the sill, signifying that the transit time from the sill to the moorings is the same as the time-lag obtained for the correlation analysis. In addition, Fig. 7 shows that following its arrival at the moorings, the tracer concentration is around 10 % to 15 % meaning that this water,

OSD
8, 1403–1440, 2011

originating from the 27.6 to 27.8 density range at the sill, comprises 10 % to 15 % of the water at the moorings. The 0.6 negative salinity anomaly present in this water at the sill in April 2004 (Fig. 5b), has most likely been diluted down to 0.06 at the moorings (Fig. 5a), by mixing with ambient downstream water masses of a higher salinity, in an approximate 9 to 1 ratio. Based on the presence of the negative salinity anomaly in OCCAM at the sill, and the results of this passive tracer experiment, we argue that hyopthesis H1 can be rejected.

5 Testing of hypotheses H2

Having identified that the 2004 negative salinity anomaly is present in OCCAM at the sill, and glacial ice-melt is not a variable present in OCCAM, hypothesis H2a can also be rejected.

It also follows that if precipitation or sea-ice melt anomalies were responsible for causing the 2004 negative salinity anomaly at the moorings, a time-lagged negative correlation would be expected between the OCCAM salinity anomaly time series at the sill, and time series of precipitation, or sea-ice melt anomalies upstream of the sill. An increased surface freshwater flux will reduce the salinity of the surface mixed layer, and these surface salinity anomalies can then propagate into the intermediate waters (150 m to 600 m) of the source regions, through wind-driven vertical turbulent diffusion at the base of the mixed layer, or deep winter convection. These anomalies might then be advected to the sill in the EGC, or the current originating in the Iceland Sea. So, a high upstream surface freshwater flux could result in a low salinity at the sill sometime later, indicated by a time-lagged negative correlation.

The only region of significant negative correlation between precipitation and OCCAM salinity is at Fram Strait (Fig. 8), with a time lag of 7 years. This suggests that the aforementioned mechanism could be causing negative salinity anomalies at the sill through increased precipitation in Fram Strait. However, passive tracer initialised at the surface in Fram Strait takes only about $2^1/_2$ years to mix with the intermediate

OSD
8, 1403–1440, 2011

layers of the EGC, and travel to the moorings (Fig. 9). Hence, the 7 year time lag is too long for this mechanism to be responsible for causing the 2004 anomaly, meaning that the negative correlation is probably due to chance. This result is unsurprising, when one considers the freshwater flux required to cause the 2004 negative salinity anomaly at the moorings. Freshwater fluxes in the Arctic and Nordic Seas can be calculated according to a reference salinity of 35.2, which represents the salinity of inflowing Atlantic Water to the Arctic Mediterranean (Dickson et al., 2007). Freshwater flux can then be calculated from the following equation:

$$F_W = V \times \left(1 - \frac{S}{S_{\mathrm{ref}}}\right) \tag{1}$$

Assuming the volume flux of the dense overflow to be 3 Sv (Dickson and Brown, 1994), and given that the UK1 salinity time series shows an average reduction in salinity from a long term mean of 34.87 to 34.84 between January 2004 and July 2004 (Fig. 3), then an increased freshwater flux at the moorings of around 3 mSv for this 6 month period would be needed to cause the anomaly. The net precipitation minus evaporation (P-E) over the whole of the Nordic Seas is only around 25 mSv (Aagaard and Carmack, 1989), and the region of strong negative correlation in Fig. 8 occupies only around 2 % of the surface area of the Nordic Seas. Therefore, only about 0.5 mSv enters this region as a result of P-E, and this would have to increase by a factor of 6, for 6 months, to provide enough freshwater to cause the anomaly. Moreover, the duration of the peak in tracer concentration at the moorings is around 1.5 years (Fig. 9), whereas the duration of the observed 2004 negative salinity anomaly is only about 6 months. This means that even in the unlikely event of an extremely high P-E input occurring capable of causing the anomaly at the moorings, the duration of its passage through the array would be too long to cause the anomaly shown in Fig. 3. Therefore hypothesis H2b is rejected on this ground as well as the unrealistic time lag, and unfeasibly high P-E requirement.

The correlation analysis between the OCCAM salinity anomaly time series at the sill and OCCAM sea-ice melt anomaly time series produced no regions of statistically

OSD
8, 1403–1440, 2011

significant correlation at any time lag, indicating that increased sea-ice melt is also probably not responsible for causing the 2004 anomaly. Around 80 mSv of sea-ice enters the Nordic Seas from the Arctic through Fram Strait (Dickson et al., 2007), and about 80 % of this melts during transit in the EGC to Denmark Strait (Aagaard and Carmack, 1989), giving a liquid freshwater input of around 64 mSv. Therefore, only a 5 % increase in sea-ice melt for a 6 month period would, in principle, provide enough freshwater to form the 2004 anomaly. So does our negative result eliminate this as a possibility, considering the relatively modest requirement of a 5 % increase? Clearly, our results show that during the time preceding the 2004 anomaly, no outstanding increase in OCCAM sea-ice melt occurred over a time period of one to several months. Even if a sufficient increase in sea-ice melt had occurred to cause the anomaly at the moorings, this freshwater would have probably remained at the surface, because of its low density, and flowed out through Denmark Strait in the surface waters of the EGC. So, this negative result can likely be accepted with a reasonable degree of confidence and consequently hypothesis H2c is rejected.

6 Testing of hypothesis H3

Given that changes in the proportion of different source waters feeding the overflow have previously been attributed to wind forcing variability (Holfort and Albrecht, 2007; Rudels et al., 2002; Rudels et al., 2003), we now see whether a statistical relationship exists between mooring UK 1 salinity data and the regional wind stress fields. A time-lagged regression analysis was performed between the UK1 salinity anomaly and NCAR 5 day mean meridional and zonal wind stress. Strong positive correlations were found between the meridional wind stress and UK1 salinity adjacent to the East Greenland coast between 72° N and 78° N (Fig. 10a). This region displayed a positive correlation for time lags ranging from 3 months to 6 months, with peak values of correlation coefficient at a lag of $4^1/_2$ months ($r = 0.53$, $p < 0.01$). Correlations between zonal wind stress and UK1 salinity showed weaker positive correlations peaking

OSD
8, 1403–1440, 2011

at the same time lag, further south across a smaller region between 70° N and 73° N (Fig. 10b). The correlation map shows that following a high southward wind stress off the east Greenland coast between about 70° N and 80° N, a reduction in salinity at the moorings occurs around $4^1/_2$ months later.

Composite sections of salinity, current velocity and sea surface height during times of positive and negative wind stress anomalies were produced at location CD at 75° N (Fig. 10b). This is the region of maximum correlation coefficient between meridional wind stress and UK1 salinity. If the composites were produced simply for the times of peak positive and negative wind stress, regardless of time of year the composites could be biased by seasonal cycles present in either the atmospheric or ocean data. Therefore, salinity, velocity and sea surface height data were extracted from OCCAM at the times shown in Fig. 5c. These times represent the three most positive and negative wind stress anomalies, occurring during each calendar month, in the de-seasoned wind stress time series displaying the highest correlation coefficient with UK1 salinity (Fig. 5c).

A wind-induced reduction in the salinity of the intermediate EGC waters (150 m to 600 m depth) feeding the overflow could be caused by stronger mixing between these water masses and the fresh overlying Polar Surface Water (PSW). An elevated input of kinetic energy to the ocean surface from a high wind stress intensifies mixing at the surface and increases the depth of the mixed layer. Wind-driven vertical turbulent diffusion, at the base of the mixed layer, could then cause the transfer of surface mixed layer fresh anomalies into the underlying halocline. These anomalies could then be advected by the EGC from the region of formation to the moorings. However, the results of the composite show that there is no statistically significant difference in the vertical salinity section at 75° N between times of strong southward and strong northward wind stress (Fig. 11a). This suggests that a wind-induced change in the salinity of the EGC is probably not responsible for freshening the overflow.

Alternatively, a stronger southward wind stress could cause a variation in the proportion of EGC water contributing to the overflow, by influencing the volume of EGC water

OSD
8, 1403–1440, 2011

transported to the sill. The velocity composite (Fig. 11b) shows a statistically significant ($p < 0.01$) increase in the southward velocity of the EGC of about $3\,\mathrm{cm\,s^{-1}}$, during times of strong southward wind stress, compared with times of strong northward wind stress. A stronger southward wind stress increases Ekman transport towards the west, causing water to pile up against the east Greenland coast. The steeper sea surface height slope (Fig. 12) creates a stronger seaward pressure gradient force (balanced by the Coriolis force), causing an increase in the southward EGC geostrophic velocity. The velocity increase is roughly uniform to a depth of about 600 m (Fig. 11b).

Can the results of the compositing exercise then explain the occurrence of the 2004 negative salinity anomaly at the moorings? Clearly, a water mass fresh enough and of the correct density to cause the anomaly would need to be present in the EGC at 75° N, and remain relatively conserved en-route to the sill. Arctic Atlantic Water (AAW), derived from the modification of Atlantic Water inflow to the Arctic, where it becomes colder and fresher, joins the EGC through Fram Strait and has the appropriate characteristics (potential density between 27.70 and 27.95, and salinity between 34.45 and 34.9) (Rudels et al., 2002). It has also been suggested that AAW is transported by a strongly barotropic EGC, steered by topography, as a distinct outflow from the Arctic through Fram Strait, flowing directly to Denmark Strait (Mauritzen, 1996; Woodgate, 1999). Moreover, it has been noted that negligible mixing occurs between the AAW, and the adjacent RAW to the east, as the two water masses flow southward from Fram Strait, forming the western limb of the wind-driven Greenland Sea Gyre (Mauritzen, 1996). Therefore, with a suitable water mass and pathway identified, a feasible mechanism could be that a stronger southward wind stress at 75° N increases the southward velocity of the EGC, increasing the volume flux of relatively fresh AAW flowing directly to the sill. This water then mixes with the other source waters immediately upstream of the sill, to form the negative anomaly that is subsequently observed at the moorings. To determine whether the timescale of water masses in the EGC to travel from location CD to the moorings, is consistent with the time lag of 4 $^1/_2$ months between wind and salinity anomalies suggested by Fig. 10, a passive tracer experiment was performed. It

OSD
8, 1403–1440, 2011

comprised an instantaneous release at section CD on grid cells with a potential density greater than 27.6, representing the density of water forming the anomaly at the sill. Tracer was released on 20 December 2003, approximately $4^1/_2$ months before the appearance of the May 2004 anomaly at the moorings. The results of this show that by 14 March 2004, the majority of the tracer is advected southward in the EGC (Fig. 13), and by 22 June 2004 it has been transported further southward to around 69° N (Fig. 13). Here, a split occurs in the tracer pathway, with some tracer being advected southwestward into Denmark Strait in the EGC, and some being advected southeastward towards the Faroe Bank Channel in the East Icelandic Current (Fig. 13). By 9 November, the tracer has reached the moorings at section AB, making the total transit time from 75° N to the moorings approximately 10 months.

So, to complete the story, an explanation is required for the 10 months taken for tracer released at 75° N to reach the moorings, compared with the $4^1/_2$ month lag between wind and salinity anomalies suggested by Fig. 10. Analysis of the volume and freshwater fluxes in the EGC at 75° N (Fig. 10b, Sect. CD), and further south at 72° N (Fig. 10b, Sect. EF) and 69° N (Fig. 10b, Sect. GH), provides an answer for this. Figure 14a and b show that the temporal variability of the vertically integrated volume and freshwater fluxes, between depths of 150 m and 600 m in the EGC at sections CD, EF and GH, are in phase at all three locations. This means that the EGC is displaying the same response to the meridional wind stress throughout most of its pathway between Fram Strait and Denmark Strait – indicative of a spinning-up of the Greenland Sea Gyre. In addition, an increase in the volume and freshwater flux at all 3 sections occurs around $4^1/_2$ months before the UK1 anomaly (Fig. 14). So the time lag of $4^1/_2$ months which produced the maximum correlation between the meridional wind stress and UK1 salinity at 75° N (Fig. 10a) is actually representing a lag of $4^1/_2$ months between a spinning-up of the Greenland Sea Gyre, and the appearance of the anomaly at the moorings. Consequently, for the results of the tracer experiment to support the proposed mechanism, there must be a transit time of $4^1/_2$ months for tracer to travel from the point where the EGC splits from the gyre, to the moorings. Figure 13 reveals that

OSD
8, 1403–1440, 2011

this is indeed the case, showing tracer separating from the gyre as a distinct southwestward flow at about 69° N, on 22 June 2004, and arriving at the moorings on 9 November 2004, a time period of approximately 4½ months. Hence we argue that hypothesis H3 can be accepted.

7 Summary

Based on the results of Sect. 6, we propose a simple mechanism responsible for causing salinity anomalies in the Angmagssalik overflow plume (Fig. 15). An elevated southward wind stress parallel to the east Greenland coast increases the circulation of the Greenland Sea Gyre. The volume flux of fresh intermediate EGC water arriving at the sill is subsequently increased, resulting in a freshening of DSOW at the Angmagssalik moorings 4½ months later.

Our results show that DSOW salinity anomalies are caused by changes in the proportions of source waters feeding the overflow, rather than changes in the salinity of the source waters. This is consistent with other relevant research (Rudels et al., 2002; Rudels et al., 2003; Holfort and Albrecht, 2007). However, in contrast with Rudels et al. (2003), we do not find evidence which supports a complete switch between source regions (EGC or the Iceland Sea) as being responsible for changes in DSOW properties. While this suggests that the EGC is a permanent source for DSOW, the variability of which is crucial in modifying the properties of DSOW, we have no evidence to eliminate the Iceland Sea as another permanent source. Our study also supports the proposed mechanism by Holfort and Albrecht (2007), who argue that stronger southward winds result in more northern, low saline water flowing towards Denmark Strait. Yet conversely, we show that it is the action of the wind over a wide area of the Nordic Seas controlling large-scale circulation, rather than the variability in the wind stress local to Denmark Strait, that modifies the salinity of the deep overflow. This means the North Atlantic Oscillation, which is the dominant factor controlling the spin-up of the Greenland Sea Gyre, could directly influence the salinity of the overflow and may have been an important contributing factor to the 30 year freshening trend seen in DSOW (Dickson et al., 2002), and its stabilisation in the last decade (Sarafanov et al., 2008). These results are significant because they highlight the importance of the EGC in modifying the salinity of DSOW. The freshening of DSOW and the associated reduction in density of NADW, could lead to a weakening of the Meridional Overturning Circulation. It is therefore essential, that climate models used to predict the response of the global thermohaline circulation to anthropogenic activity accurately represent the structure and variability of the EGC, and its response to regional atmospheric forcing. The presence of a weaker EGC within the model may result in an absence of DSOW salinity anomalies, and future changes in the global thermohaline circulation may not be identified.

Acknowledgements. We thank Andrew Coward and the OCCAM team at the National Oceanography Centre, Southampton, for their help and providing the model data. The research presented in this paper was carried out on the High Performance Computing Cluster supported by the Research Computing Service at the University of East Anglia. The research leading to these results has received funding from the European Community's 7th framework programme (FP7/2007-2013) under grant agreement No. GA212643 (THOR: "Thermohaline Overturning – at Risk", 2008-2012) and from Defra projects SD0440 & ME5102. We thank the many chief scientists and crew completing the annual deployment of the Angmagssalik Array, and acknowledge the contributions of the University of Hamburg and The Finnish Institute of Marine Research. SH was funded by a NERC CASE award at the University of East Anglia supported by Cefas project DP239.

OSD
8, 1403–1440, 2011

References

Aagaard, K. and Carmack, E.: The Role of Sea Ice and Other Fresh Water in Arctic Circulation, J. Geophys. Res., 94, 14485–14498, 1989.

Coward, A. and de Cuevas, B.: The OCCAM 66 Level Model: physics, initial conditions and external forcing, SOC Internal Report No. 99, National Oceanography Centre, Southampton, UK, 2005.

Curry, R., Dickson, B., and Yashayaev, I.: A change in the freshwater balance of the Atlantic Ocean over the past four decades, Nature, 426, 826–829, 2003.

Dickson, R. R. and Brown, J.: The production of North Atlantic Deep Water: Sources, rates and pathways, J. Geophys. Res., 99, 12319–12341, 1994.

Dickson R. R., Yashayaev, I., Meincke, J., Turrell, W. R., Dye, S. R., and Holfort, J.: Rapid Freshening of the Deep North Atlantic over the past Four Decades, Nature, 416, 832–837, 2002.

Dickson, R. R., Rudels, B., Dye, S., Karcher, M., Meincke, J., and Yashayaev, I.: Current estimates of freshwater flux through Arctic and subarctic seas, Prog. Oceanogr., 73, 210–230, 2007.

Dickson, R. R., Dye, S. R., Jonsson, S., Köhl, A., Macrander, A., Marnela, M., Meincke, J., Olsen, S., Rudels, B., Valdimarsson, H., and Voet, G.: The overflow flux west of Iceland: variability, origins and forcing in Arctic-Subarctic Ocean Fluxes, edited by: Dickson, R. R., Meincke, J., and Rhines, P., Chapter 19, 443–474, doi:10.1007/978-1-4020-6774-7_20, 2008.

Fogelqvist, E., Blindheim, J., Tanhua, T., Østerhus, S., Buch, E., and Rey, F.: Greenland-Scotland overflow studied by hydro-chemical multivariate analysis, Deep-Sea Res. Pt. I, 50, 73–102, 2003.

Hansen, B. and Østerhus, S.: North Atlantic – Nordic Seas exchanges, Prog. Oceanogr., 45, 109–208, 2000.

Holfort, J. and Albrecht, T.: Atmospheric forcing of DSOW salinity, Ocean Sci., 3, 411–416, 2007, http://www.ocean-sci.net/3/411/2007/.

Holliday, N., Meyer, A., Bacon, S., Alderson, G., and de Cuevas, B.: Retroflection of part of the East Greenland Current at Cape Farewell, Geophys. Res. Lett., 34, L07609, doi:10.1029/2006GL029085, 2007.

OSD
8, 1403–1440, 2011

Wind forcing of salinity anomalies in the Denmark Strait overflow

S. Hall et al.

Jónsson, S. and Valdimarsson, H.: A new path for the Denmark Strait overflow water from the Iceland Sea to Denmark Strait, Geophys. Res. Lett., 31(3), L03305, doi:10.1029/2003GL019214, 2004.
Kalnay, E., Kanamitsu, M., Kistler, R., Collins, W., Deaven, D., Gandin, L., Iredell, M., Saha, S., White, G., Woollen, J., Zhu, Y., Chelliah, M., Ebisuzaki, W., Higgins, W., Janowiak, J., Mo, K., Ropelewskia, C., Leetmaa, A., Reynolds, R., and Jenne, R.: The NCEP/NCAR reanalysis project, Bull. Amer. Meteor. Soc., 77, 437–495, 1996.
Köhl, A.: Variable source regions of Denmark Strait and Faroe Bank Channel overflow waters, Tellus Series A: Dynamic Meteorology and Oceanography, ISSN: 02806495, 62, 551–569, 2010.
Mauritzen, C.: Production of dense overflow waters feeding the North Atlantic across the Greenland-Scotland Ridge, Part 1. Evidence for a revised circulation scheme, Deep-Sea Res. PT. I, 43, 769–806, 1996.
Pawlowicz, R., Beardsley, B., and Lentz, S.: Classical tidal harmonic analysis including error estimates in MATLAB using T TIDE, Comput. Geosci., 28, 929–937, 2002.
Peterson, B., McClelland, J., Curry, R., Holmes, R., Walsh, J., and Aagaard, K.: Trajectory Shifts in the Arctic and Subarctic Freshwater Cycle, Science, 313, 1061–1066, 2006.
Pickart, R., Torres, D., and Fratantoni, P.: The East Greenland spill jet, J. Phys. Oceanogr., 35, 1037–1053, 2005.
Quadfasel, D.: Summary Cruise Report R/V MARIA S. MERIAN Cruise MSM12-1, Institut für Meereskunde, KlimaCampus, Universität Hamburg, Bundesstr. 53, D-20146 Hamburg, 2009.
Rudels, B., Fahrbach, E., Meincke, J., Budeus, G., and Eriksson, P.: The East Greenland Current and its contribution to the Denmark Strait overflow, J. Mar. Sci., 59, 1133–1154, 2002.
Rudels, B., Eriksson, P., Buch E., Budéus, G., Fahrbach, E., Malmberg, S.-A., Meincke, J., and Mälkki, P.: Temporal switching between sources of the Denmark Strait overflow water, ICES Mar. Sci. Symp., 219, 319–325, 2003.
Sarafanov, A., Falina, A., Sokov, A., and Demidov, A.: Intense warming and salinification of intermediate waters of southern origin in the eastern subpolar North Atlantic in the 1990s to mid-2000s, J. Geophys. Res., 113:C12022, doi:10.1029/2008JC004975, 2008.
Saunders, P. M.: The dense northern overflows, in: Ocean circulation and climate, edited by: Siedler, G., Church, J., Gould, J., Academic Press Int. Geophys. Ser., 77, 401–417, 2001.

OSD
8, 1403–1440, 2011

Wind forcing of salinity anomalies in the Denmark Strait overflow

S. Hall et al.

Saunders, P. M., Cunningham, S., de Cuevas, B., and Coward, A.: Comments on "Decadal Changes in the North Atlantic and Pacific Meridional Overturning Circulation and Heat Flux", J. Phys. Oceanogr., 38, 2104–2107, 2008.
Voet, G. and Quadfasel, D.: Entrainment in the Denmark Strait overflow plume by mesoscale eddies, Ocean Sci., 6, 301–310, 2010, http://www.ocean-sci.net/6/301/2010/.
Walter, M., Mertens, C., and Rhein, M.: Mixing estimates from a large-scale hydrographic survey in the North Atlantic, Geophys. Res. Lett., 32, L13605, doi:10.1029/2005GL022471, 2005.
Woodgate, R., Fahrbach, E., and Rohardt, G.: Structure and transport of the East Greenland Current at 75° N from moored current meters, J. Geophys. Res., 104, 18059–18072, 1999.

OSD
8, 1403–1440, 2011

Table 1. Locations, depths and deployment dates of moorings in (2).

Mooring	Location	Instrument depth (m)	Height above sea bed (m)	Water depth (m)	Deployment dates
F2	63.55° N 36.50° W	1760	20	1780	15 July 2003 to 27 July 2005
UK1	63.48° N 36.29° W	1970	20	1990	24 August 1998 to 19 August 1999 10 August 2000 to 1 July 2001
G1	63.37° N 36.07° W	2180	20	2200	10 August 2000 to 13 June 2002
UK2	63.27° N 35.87° W	2350	18	2368	15 July 2003 to 27 July 2005

OSD
8, 1403–1440, 2011

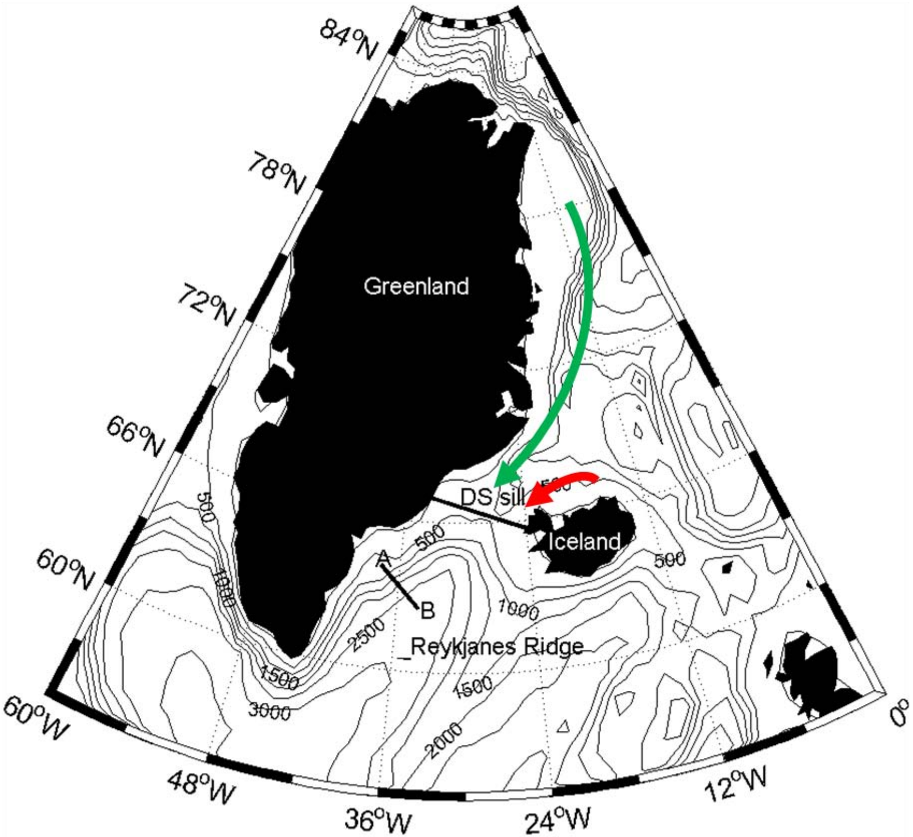

Fig. 1. Map showing the Denmark Strait overflow sill (DS sill) and the Angmagssalik mooring array (section AB). All isobaths are in metres. DSOW source pathways: EGC (green), Iceland Sea (red).

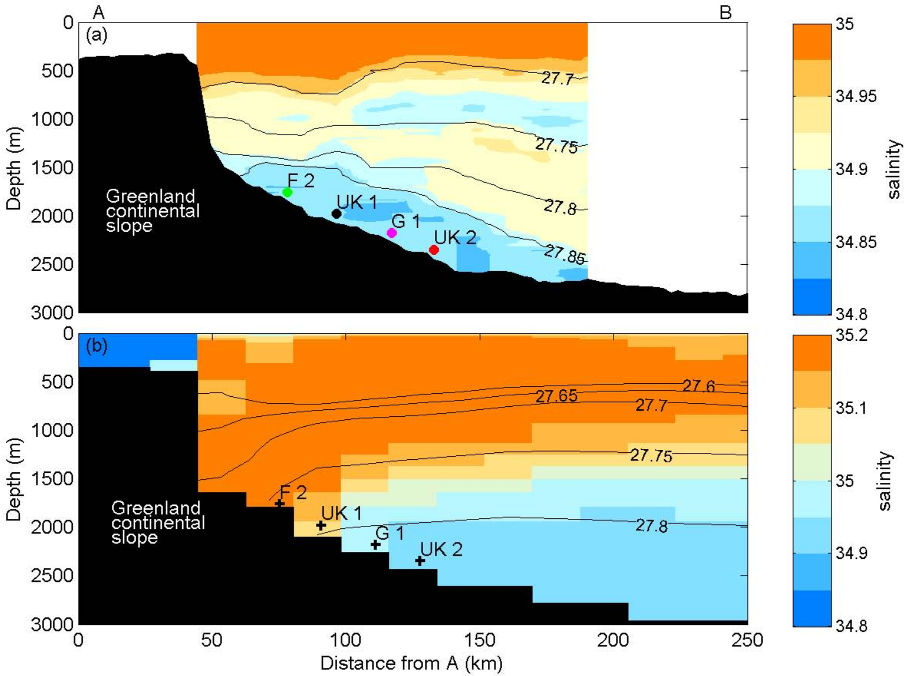

Fig. 2. (a) Vertical profile of section AB showing the moorings F2, UK1, G1 and UK2 positioned on the East Greenland continental slope, at the depths at which salinity measurements were obtained. Contours and shading represent potential density and salinity respectively, obtained from CTD casts during the June 2009 MSM 12-1 cruise. **(b)** Section through the Angmagssalik moorings in OCCAM, showing the mean June OCCAM salinity between 1994 and 2004. Contours indicate the 11-year mean of OCCAM potential density. Note the different colour bar scales in each figure.

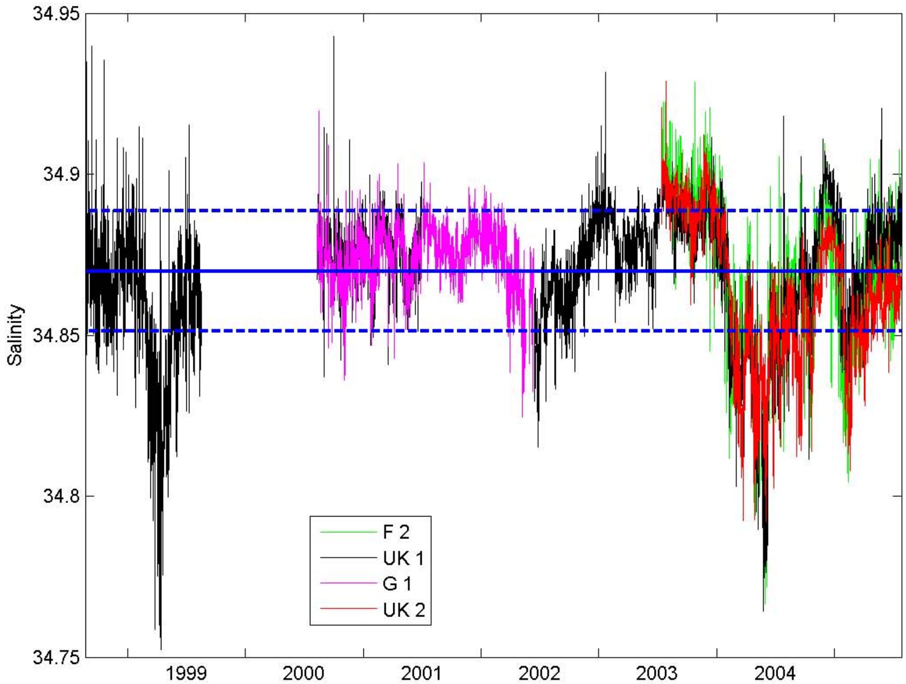

Fig. 3. Salinity time series from the Angmagssalik array Sea-Bird MicroCATs (Dickson et al., 2008). Data have been binned into 1 h means from the original 10 min sampling rate. Solid blue line represents the mean of the time series, and dotted blue lines represent plus and minus 1 standard deviation. Tidal signals have been removed.

OSD
8, 1403–1440, 2011

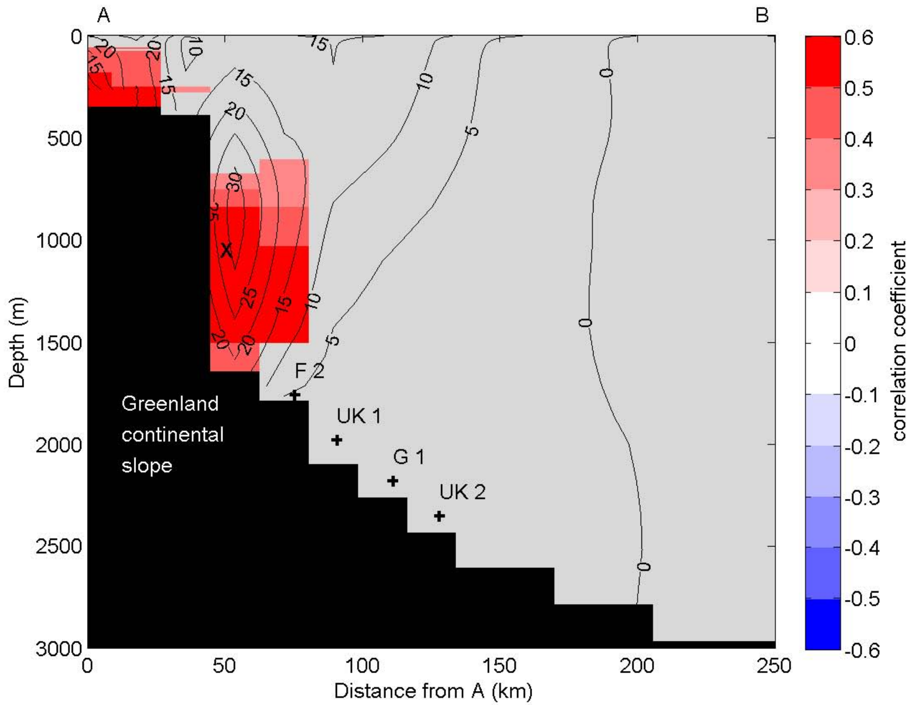

Fig. 4. Section through the Angmagssalik moorings in OCCAM, showing the correlation coefficient between mooring UK1 salinity anomaly time series shown in (5a), and the equivalent OCCAM salinity anomaly time series in each grid cell ($p < 0.01$). Contours indicate the 11-year mean of OCCAM current velocity ($\mathrm{cm\,s^{-1}}$) normal to section AB (positive values indicate southwestward flow). Grey indicates no statistically significant correlation.

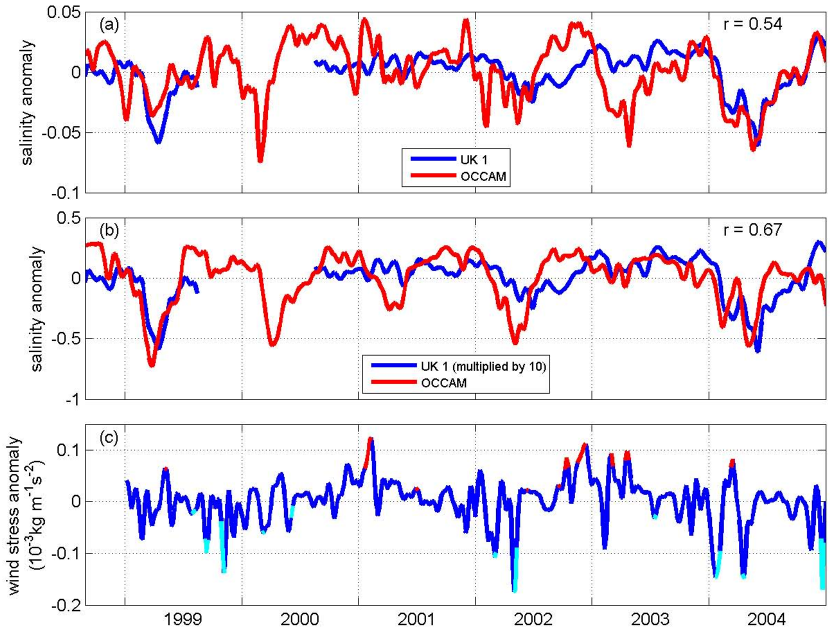

Fig. 5. **(a)** UK 1 (blue) and OCCAM (red) salinity anomaly time series. OCCAM time series taken from location marked "X" in (4). For the whole time series, the correlation coefficient $r = 0.54$, for 2004 only, $r = 0.96$ ($p < 0.01$). **(b)** UK 1 (blue) and OCCAM (red) salinity anomaly time series. OCCAM time series taken from location marked "+" in (6). The maximum value of $r = 0.67$ ($p < 0.01$) occurs for a time lag of 6 weeks. UK 1 time series multiplied by a factor of 10 to allow direct comparison of both time series. **(c)** NCAR meridional wind stress anomaly at the grid cell of highest correlation ($r = 0.53$, $p < 0.01$) at 75° N 20° W in (10a). A time lag of 4.5 months has been applied to the time series. Seasonal cycle has been removed. Red and cyan indicate the three maximum (red) and minimum (cyan) wind stress anomalies, for each calendar month, over the 6 year period - used for compositing salinity, velocity and sea surface height.

OSD
8, 1403–1440, 2011

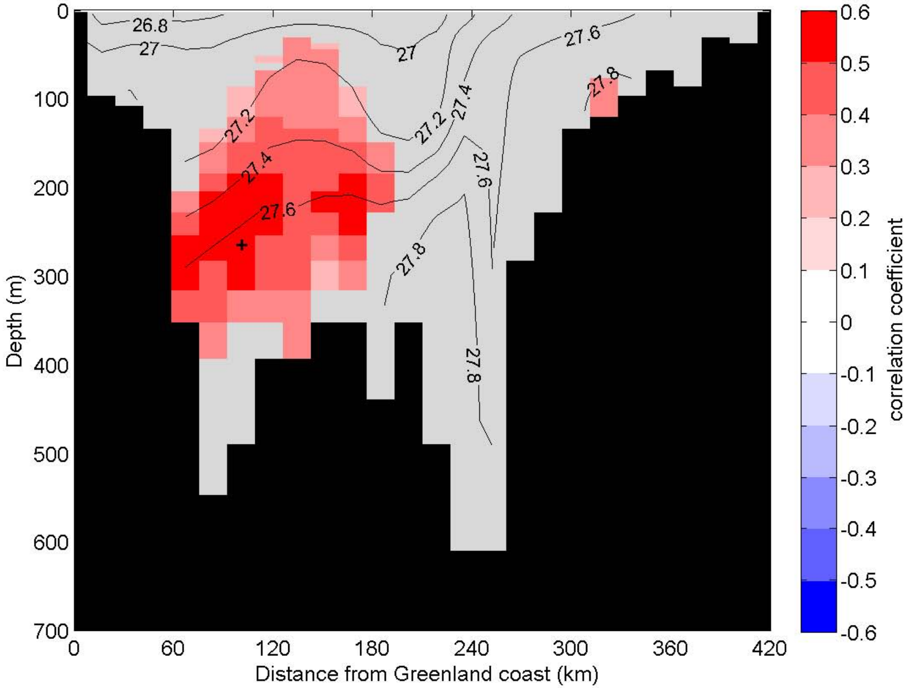

Fig. 6. Section through the overflow sill in OCCAM, showing the correlation coefficient between mooring UK 1 salinity anomaly time series, and the equivalent OCCAM salinity anomaly time series in each grid cell ($p < 0.01$). Contours indicate the 11-year mean of OCCAM potential density. Grey indicates no statistically significant correlation.

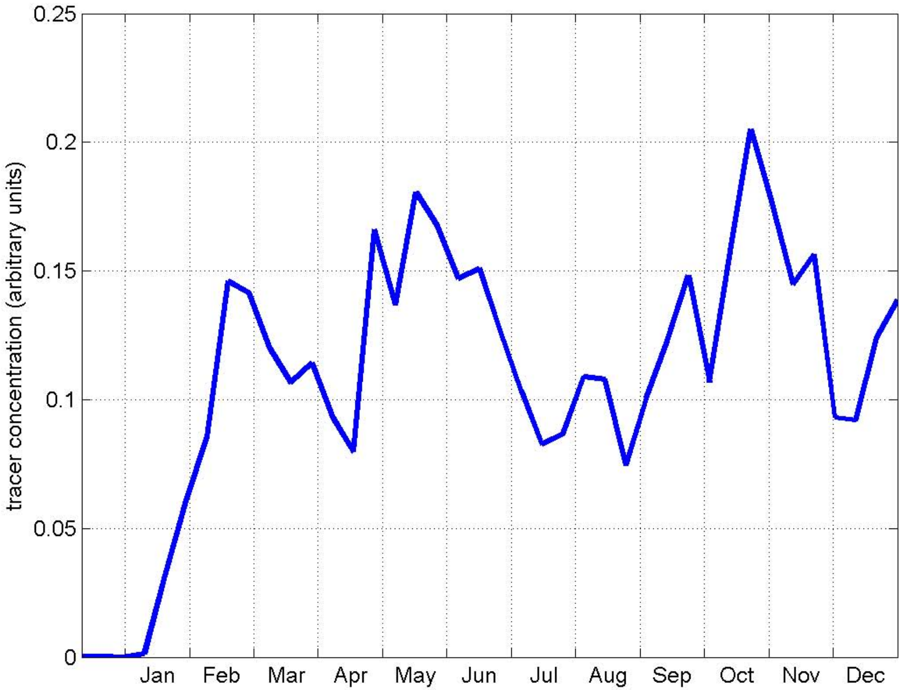

Fig. 7. Time series of passive tracer concentration at the OCCAM location of the overflow at the moorings, taken from grid cell at location marked "X" in (4). Passive tracer was initialised at the sill on grid cells with a potential density between 27.6 and 27.8, on 12 December 2003, and continuously released until 31 December 2004. This water mass constitutes around 10–15 % of the water present at location "X".

OSD
8, 1403–1440, 2011

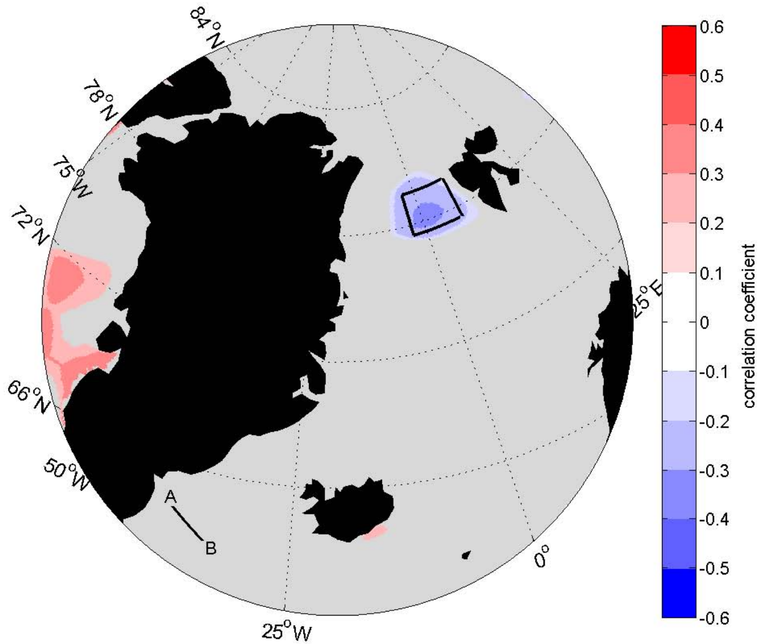

Fig. 8. Map of the time-lagged correlation coefficient between an 11 year time series (1994 to 2004) of the OCCAM sill salinity anomaly time series shown in (5b), and a 1994 to 2004 time series of CMAP 5 day mean precipitation (extracted from OCCAM) ($p < 0.01$). Time lag is 7 years. Grey indicates no statistically significant correlation. Boxed area indicates region of passive tracer release.

OSD
8, 1403–1440, 2011

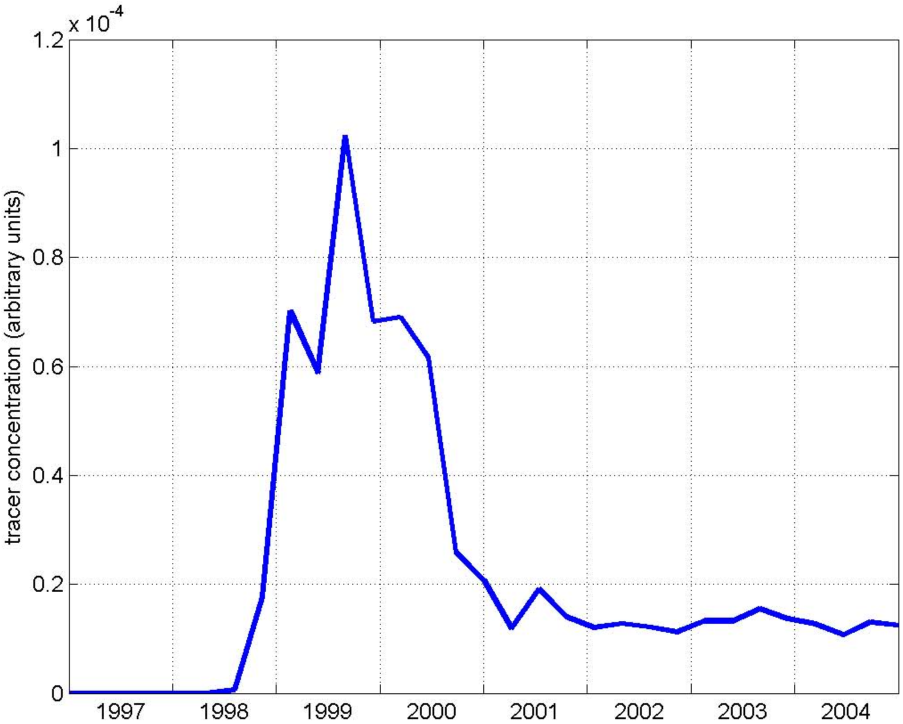

Fig. 9. Time series of passive tracer concentration at the OCCAM location of the overflow at the moorings, taken from grid cell at location marked "X" in (4). Passive tracer was initialised at the surface in January 1997, and instantaneously released across the boxed region in (8).

OSD
8, 1403–1440, 2011

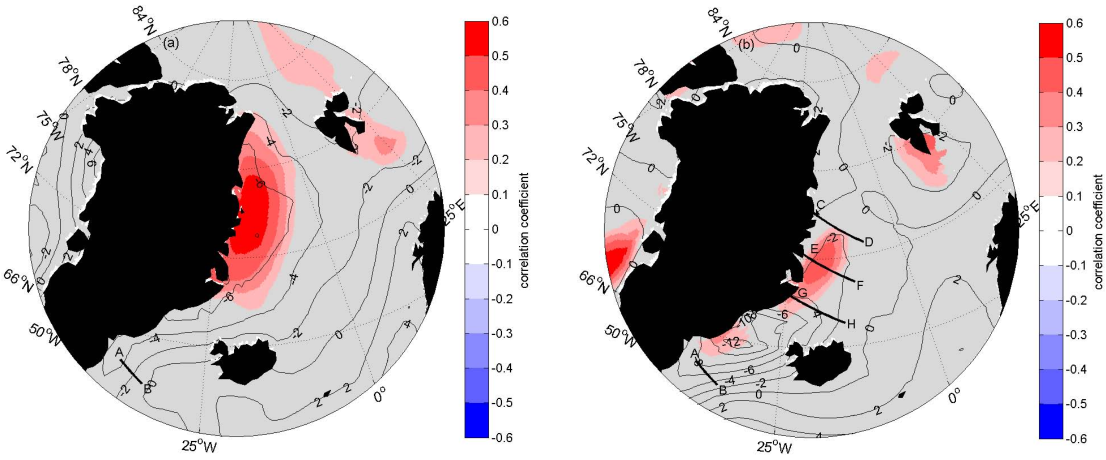

Fig. 10. Maps of the time-lagged correlation coefficient ($p < 0.01$) between mooring UK1 salinity anomaly time series shown in (5a), and NCAR 5 day mean meridional wind stress (**a**) and zonal wind stress (**b**) Time lag is $4\frac{1}{2}$ months. Contours indicate the 11-year mean of NCAR meridional and zonal wind stress ($10^{-3}\,\mathrm{kg\,m^{-1}\,s^{-2}}$). Grey indicates no statistically significant correlation. CD, EF and GH are sections used to calculate the volume and freshwater flux of the EGC.

OSD
8, 1403–1440, 2011

Wind forcing of salinity anomalies in the Denmark Strait overflow

S. Hall et al.

Title Page
Abstract Introduction
Conclusions References
Tables Figures
◀I ▶I
◀ ▶
Back Close
Full Screen / Esc
Printer-friendly Version
Interactive Discussion

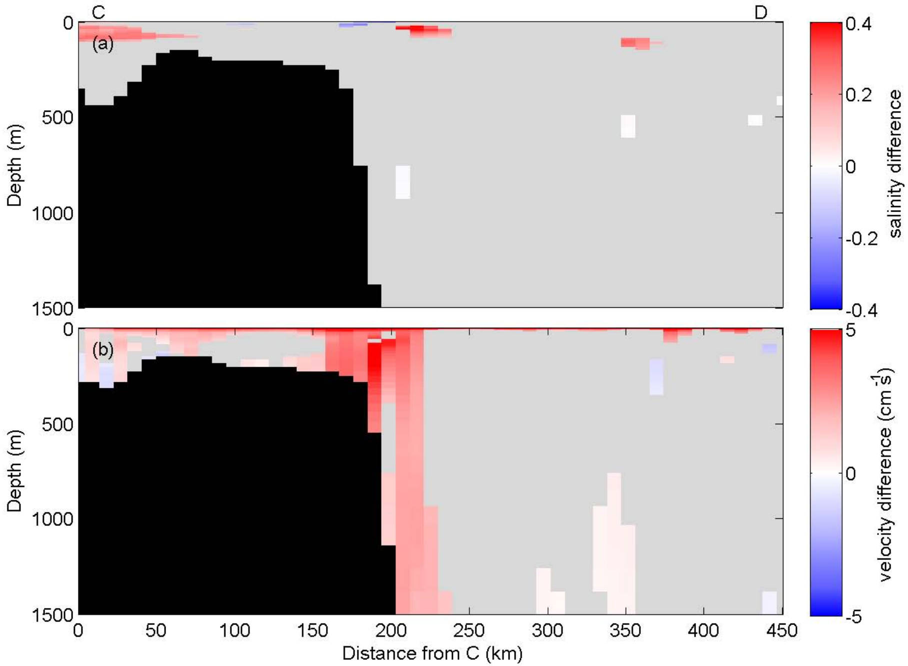

Fig. 11. Difference in salinity **(a)**, and velocity **(b)** across section CD, between times of strong positive and strong negative wind stress anomalies. Seasonal effects have been removed, by compositing the salinity and velocity data from 6 samples taken from every calendar month between 1999 and 2004 (full description in text). Grey indicates no statistically significant difference ($p < 0.01$).

OSD
8, 1403–1440, 2011

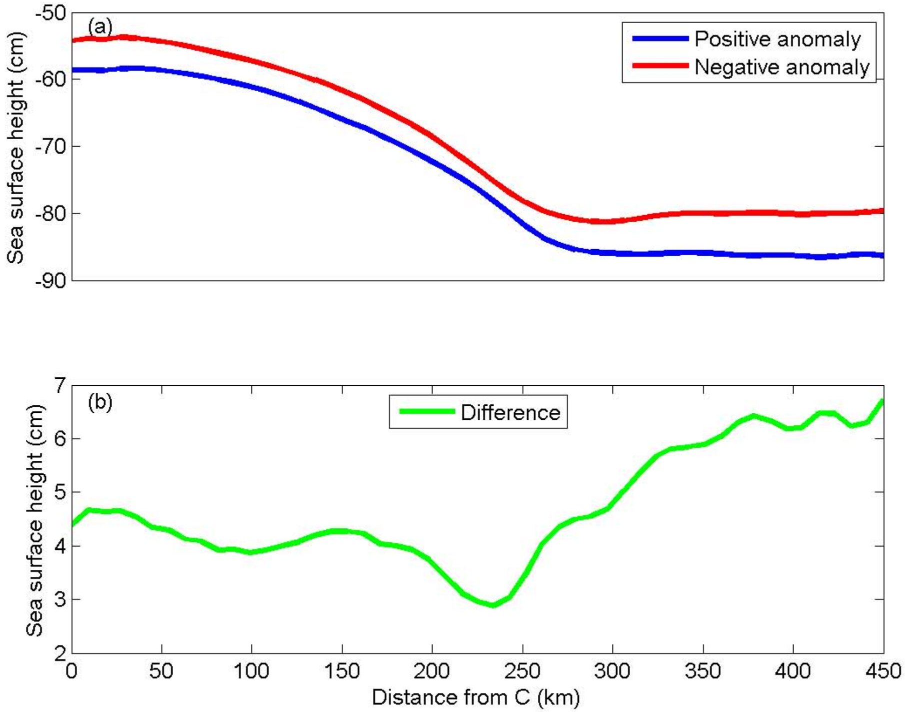

Fig. 12. **(a)** Sea-surface height across section CD during times of strong positive, and strong negative wind stress anomalies. Their difference is plotted in **(b)**. Seasonal effects have been removed, by compositing the sea-surface height data from 6 samples taken from every calendar month between 1999 and 2004 (full description in text). The offset is due to the reduced atmospheric pressure during times of strong negative wind stress anomalies. The difference is statistically significant ($p < 0.01$).

OSD
8, 1403–1440, 2011

Title Page
Abstract | Introduction
Conclusions | References
Tables | Figures
◀| |▶
◀ ▶
Back | Close
Full Screen / Esc
Printer-friendly Version
Interactive Discussion

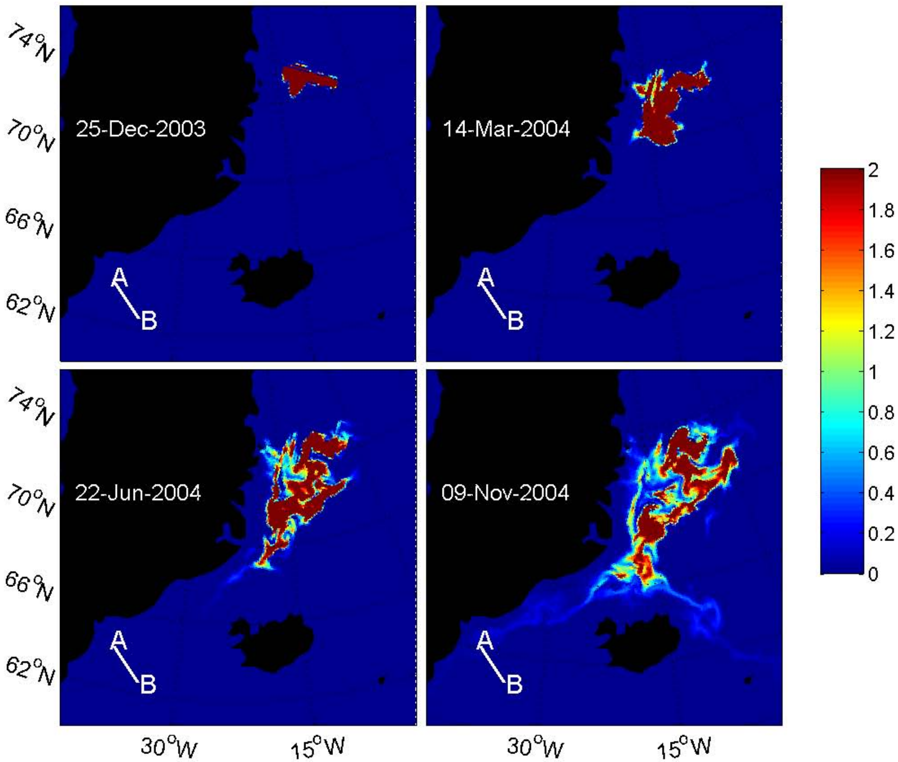

Fig. 13. Time-evolution of passive tracer, instantaneously released on 20 December 2003 across section CD. Tracer was initialised on grid cells with potential density greater than 27.6. Colour bar indicates vertically integrated tracer concentration in arbitrary units.

OSD
8, 1403–1440, 2011

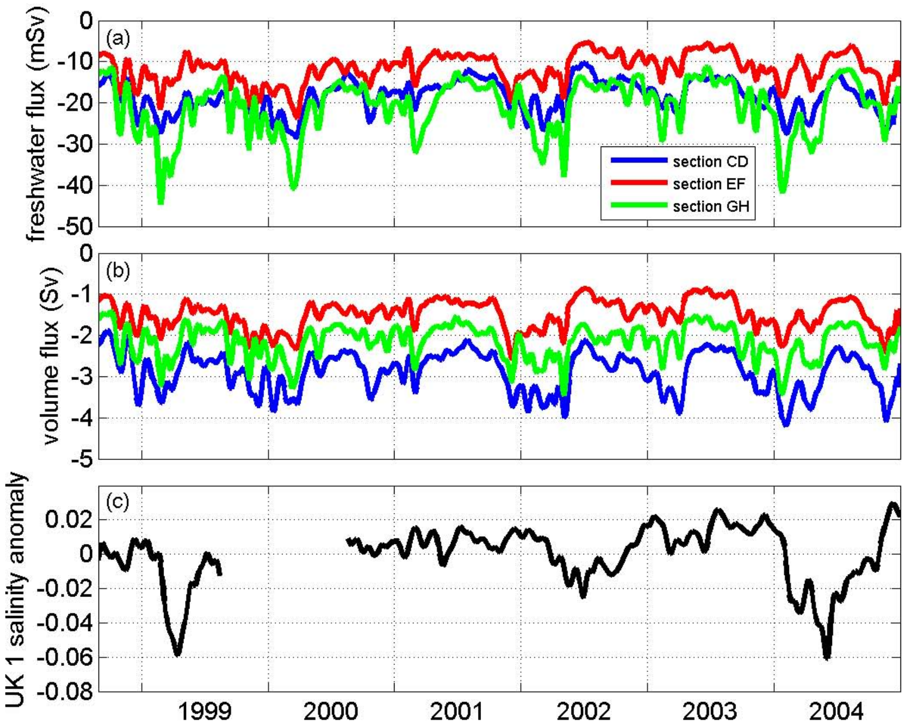

Fig. 14. Time series of freshwater flux **(a)** and volume flux **(b)**, across sections CD, EF and GH shown in (10b). Freshwater flux has been calculated relative to a reference salinity of 35.2. Freshwater flux and volume flux have been integrated between depths of 150 m and 600 m, to correspond with the depth of the Intermediate EGC water feeding the overflow. UK1 salinity anomaly time series is shown in **(c)**.

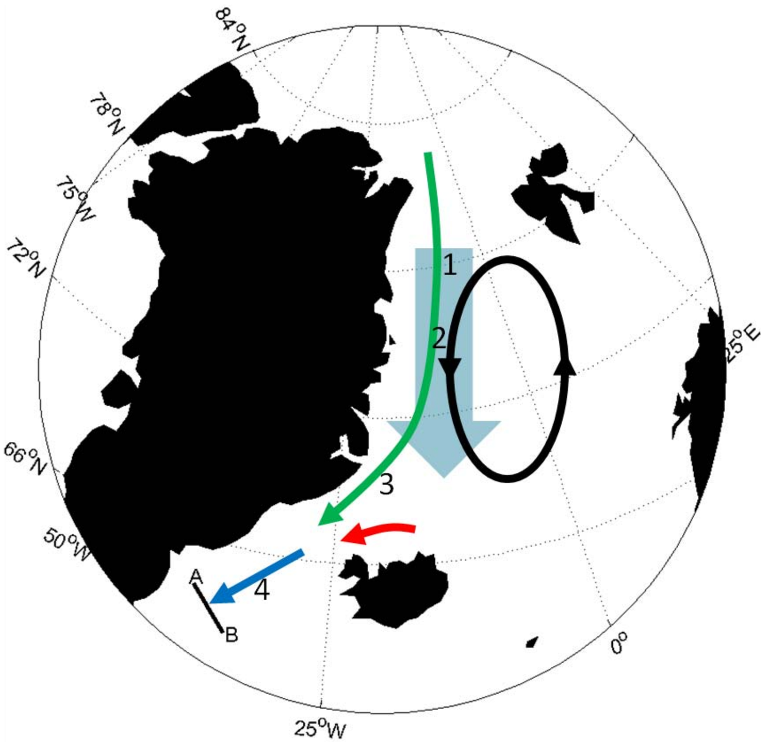

Fig. 15. The mechanism controlling salinity anomalies at the Angmagssalik moorings (Sect. AB). (1) Southward wind stress increases. (2) Greenland Sea Gyre circulation increases. (3) Increase in volume flux of fresh intermediate EGC water arriving at the sill. (4) Freshening of Denmark Strait Overflow Water. Total time for whole process is $4^1/_2$ months.